



Article

Organ Segmentation and Phenotypic Trait Extraction of Cotton Seedling Point Clouds Based on a 3D Lightweight Network

Jiacheng Shen ¹, Tan Wu ¹, Jiaxu Zhao ¹, Zhijing Wu ², Yanlin Huang ¹, Pan Gao ^{1,*} and Li Zhang ^{1,*}

¹ College of Information Science and Technology, Shihezi University, Shihezi 832061, China; shenjiacheng157@gmail.com (J.S.); rutubet4994@gmail.com (T.W.); zdgmdfzr@gmail.com (J.Z.); ylh81486@gmail.com (Y.H.)

² College of Economics and Management, Shihezi University, Shihezi 832061, China; endless731@outlook.com

* Correspondence: gp_inf@shzu.edu.cn (P.G.); zl_inf@shzu.edu.cn (L.Z.)

Abstract: Cotton is an important economic crop; therefore, enhancing cotton yield and cultivating superior varieties are key research priorities. The seedling stage, a critical phase in cotton production, significantly influences the subsequent growth and yield of the crop. Therefore, breeding experts often choose to measure phenotypic parameters during this period to make breeding decisions. Traditional methods of phenotypic parameter measurement require manual processes, which are not only tedious and inefficient but can also damage the plants. To effectively, rapidly, and accurately extract three-dimensional phenotypic parameters of cotton seedlings, precise segmentation of phenotypic organs must first be achieved. This paper proposes a neural network-based segmentation algorithm for cotton seedling organs, which, compared to the average precision of 75.4% in traditional unsupervised learning, achieves an average precision of 96.67%, demonstrating excellent segmentation performance. The segmented leaf and stem point clouds are used for the calculation of phenotypic parameters such as stem length, leaf length, leaf width, and leaf area. Comparisons with actual measurements yield coefficients of determination R^2 of 91.97%, 90.97%, 92.72%, and 95.44%, respectively. The results indicate that the algorithm proposed in this paper can achieve precise segmentation of stem and leaf organs, and can efficiently and accurately extract three-dimensional phenotypic structural information of cotton seedlings. In summary, this study not only made significant progress in the precise segmentation of cotton seedling organs and the extraction of three-dimensional phenotypic structural information, but the algorithm also demonstrates strong applicability to different varieties of cotton seedlings. This provides new perspectives and methods for plant researchers and breeding experts, contributing to the advancement of the plant phenotypic computation field and bringing new breakthroughs and opportunities to the field of plant science research.



Citation: Shen, J.; Wu, T.; Zhao, J.; Wu, Z.; Huang, Y.; Gao, P.; Zhang, L. Organ Segmentation and Phenotypic Trait Extraction of Cotton Seedling Point Clouds Based on a 3D Lightweight Network. *Agronomy* **2024**, *14*, 1083. <https://doi.org/10.3390/agronomy14051083>

Academic Editor: Gniewko Niedbała

Received: 19 April 2024

Revised: 10 May 2024

Accepted: 16 May 2024

Published: 20 May 2024



Copyright: © 2024 by the authors. Licensee MDPI, Basel, Switzerland. This article is an open access article distributed under the terms and conditions of the Creative Commons Attribution (CC BY) license (<https://creativecommons.org/licenses/by/4.0/>).

1. Introduction

Cotton is the world's leading fiber and oilseed crop, providing approximately 35% of the fiber used by humans [1] and playing a crucial role in the global economy [2]. Currently, the global area under cotton cultivation, as well as production, consumption, and stock levels, are on an upward trend [3]. As the largest producer of raw cotton in the world [4], China's cotton output is directly linked to the livelihoods of its farmers [5]. While China has a wide variety of cotton species, there is a lack of varieties suited for mechanical harvesting, leading to increased planting costs and severely restricting the healthy development of the cotton industry in the country. The breeding and selection of cotton varieties is thus an urgent issue to address.

Plant phenotyping is crucial for breeders to select the desired genotypes. The phenotypic characteristics of cotton seedlings can visually reflect their nutritional status and susceptibility to pests and diseases; therefore, research into automatic observation techniques during the cotton seedling stage is of great importance [6]. The question of how to

conduct phenotypic observations efficiently, non-destructively, and on a large scale has become a significant topic. Parameters such as leaf length, width, area, and stem length are vital indicators for monitoring plant growth and predicting yield [7]. This study selects these parameters as the focus of research, aiming to provide robust data support for cotton breeding through precise measurement and analysis.

Traditional methods of phenotypic information acquisition primarily involve manual measurements, which often damage the plant's own structure, are time-consuming, labor-intensive, inefficient, and difficult to scale, thus failing to ensure accuracy [8]. Additionally, traditional measurement techniques are limited by the tools used and environmental conditions, making it challenging to achieve large-scale, high-precision measurements. In recent years, plant phenotyping research has mainly focused on the two-dimensional aspect. Zhang Weizheng et al. [9] developed a method for segmenting maize plant images based on skeleton extraction and binary tree analysis, yet it still fails to capture leaf length, leaf curvature, or intersecting leaves. Bylesjö et al. [10] developed a tool for automatically analyzing leaf images, providing an efficient and accurate method to analyze leaf area, but it still does not reflect the overall phenotypic structure of plants. Dhondt, S, under the LAMINA framework, as well as others [11], have researched plant phenotyping systems imaging programs by focusing on spatial and temporal resolution. Lee et al. [12] used a classifier developed with a superpixel-based machine learning algorithm to precisely segment large-scale plant image datasets. Ji et al. [13] monitored the entire growth period of faba bean plants using UAV imagery to measure plant height. However, although these studies have achieved certain successes, due to characteristics such as spatial self-occlusion of the plants, acquiring two-dimensional phenotypic information from digital images cannot meet the current needs of breeding [14]. Consequently, the acquisition of three-dimensional structural phenotypic information is increasingly valued [15], making the acquisition and analysis of three-dimensional structural phenotypic information a current research bottleneck.

Currently, the acquisition of three-dimensional phenotypic information primarily focuses on the processing and analysis of three-dimensional point cloud data. Miao, T. et al. [16] proposed a method for automatically segmenting corn seedling point clouds to isolate tender corn branches and leaves. Wang Chuanyu et al. [17] used a binocular stereo-vision system to measure the three-dimensional coordinates of corn leaves, assembling them into complete leaves through three-dimensional surface stitching. Lai Yibin and others [18] proposed a three-dimensional point cloud segmentation method tailored for plants, based on the characteristics of plant point clouds. Meanwhile, the integration of plant high-throughput methods with three-dimensional structural phenotyping has been increasingly emphasized in recent years. Fahlgren, N. et al. [19] noted that a key advancement in high-throughput phenotyping platforms is the ability to non-destructively capture plant traits. Chen, D.J., and others [20] indicated that the systematic quantification of phenotypic traits or their components through high-throughput methods remains a significant challenge.

In conclusion, numerous scholars have conducted observations on crops such as corn [21], rice [22], wheat [23], and soybeans [24]. However, due to the complex structure of cotton seedlings, there has been limited research on the three-dimensional phenotyping of cotton seedlings to date. Therefore, this paper addresses the issues of complex structures during the cotton seedling stage and the lack of a clear method for three-dimensional measurement. We propose an organ segmentation and phenotypic trait extraction of cotton seedling point clouds based on a 3D lightweight network, where the collected point cloud data are preprocessed and annotated before being segmented in a hybrid network model. Subsequently, the segmented leaf and stem point clouds are used for calculating various phenotypic parameters. This research method offers new perspectives and approaches for plant researchers and breeding experts, contributing to the advancement of the field of plant phenotypic computation. By precisely extracting and analyzing three-dimensional phenotypic structural information of plants, researchers can gain a deeper understanding

of plant growth and development. This supports the optimization of breeding decisions, enhancing crop yield and variety improvement.

The main contributions of this paper are as follows:

- (1) Two varieties of cotton, Xinluzao 1 and Xinluzao 76, were cultivated, and 3D point cloud models of these cotton seedlings were successfully constructed and produced as a dataset.
- (2) This paper introduces a segmentation algorithm that combines the PointNet++ neural network with improved region-growing techniques. This hybrid approach effectively extracts local features of cotton seedlings and facilitates accurate segmentation of key organs. It outperforms traditional machine learning methods, providing a more efficient and accurate approach to plant phenotyping.
- (3) The segmented cotton seedling organs underwent phenotypic parameter calculations, revealing a strong linear relationship between the calculated and true values with minimal error. This demonstrates the method's ability to efficiently and non-destructively extract key phenotypic parameters, providing robust technical support for breeding experts and researchers, and making a significant contribution to the field of plant phenotyping.

2. Materials and Methods

2.1. Experimental Material

This experiment was conducted at the Agricultural Experiment Station of Shihezi University, located at longitude $85^{\circ}9'51.231''$ E and latitude $44^{\circ}35'47.720''$ N, where cotton cultivation and point cloud data collection were performed. The study focused on the Xinluzao 1 variety of cotton, which was cultivated in a controlled environment to enable precise observation of its growth. Point cloud data collection was specifically carried out during the cotton seedling stage. The Xinluzao 1 variety typically progresses from germination to the seedling stage within an average growth cycle of 7 days. During this period, the indoor temperature was maintained at 23°C , and the relative humidity was controlled at 25%, providing stable environmental conditions for the growth of the cotton seedlings.

To validate the applicability of the algorithm proposed in this paper across different environments and cotton varieties, the Xinluzao 76 variety of cotton was also cultivated as a control experiment. In this control experiment, the indoor temperature was adjusted to 25°C , and the relative humidity was maintained at 35% to simulate different environmental conditions. By collecting and analyzing the point cloud data of these two cotton varieties, the segmentation efficiency of the algorithm under varying conditions can be assessed, thereby verifying its generalizability.

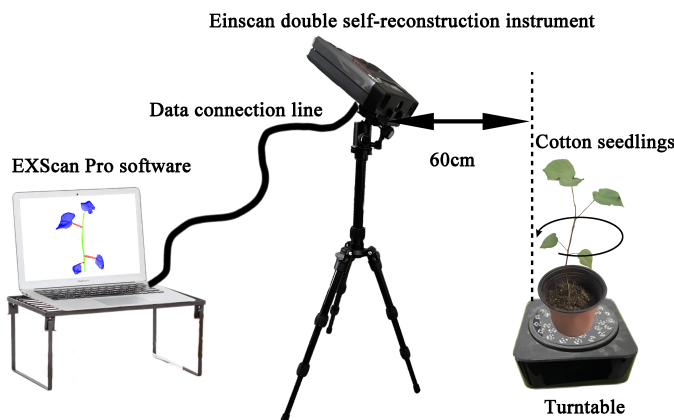
2.2. Data Acquisition System Construction

Due to the occlusion problem among crop leaves, images from a single viewpoint often fail to provide complete crop information. To address this issue, a cotton seedling point cloud acquisition system was developed. The system consists of an EinScan binocular reconstruction instrument, a laptop computer, an electric turntable, coils, and a tripod. The detailed specifications of the binocular reconstruction instrument are shown in Table 1; the scanner offers a point accuracy of up to 0.1 mm and a point spacing ranging from 0.2 mm to 3 mm. This high resolution is crucial for capturing the complex details of cotton seedlings.

Table 1. EinScan detailed specifications.

Parameters	Values
scan precision	0.1 mm
point spacing	0.2 mm–3 mm
single-scan coverage	150 mm × 120 mm–250 mm
scan depth	300 mm–500 mm
baseline working distance	400 mm

To precisely capture the surface features and details of cotton seedlings and obtain high-quality point cloud data, the plant is positioned at the center of the turntable. The binocular reconstruction instrument is mounted on the tripod, directly facing the center of the turntable. By connecting the binocular reconstruction instrument to the laptop and employing a white LED light source combined with structured light scanning technology, three-dimensional point cloud information of the cotton seedlings is collected. Additionally, depending on the complexity of the cotton plant phenotypes, the rotation speed of the turntable is controlled between 8 to 15 revolutions per minute. Slow rotation helps reduce motion blur caused by fast movements and allows more data points to be gathered in overlapping areas, enhancing the accuracy of the point cloud reconstruction and reducing errors during the reconstruction process. This setup captures the surface details of the plant more accurately, taking an average of 3 min to obtain the point cloud data for each plant. Finally, the collected data are automatically registered and fused using ExScan Pro v4.0 software, outputting the cotton seedling point cloud data. The setup is illustrated in Figure 1, which displays the point cloud data collection system.

**Figure 1.** Data acquisition system.

This experiment utilized a three-dimensional point cloud acquisition system for cotton seedlings to collect data from 100 healthy cotton seedlings during their early growth stages. Before the experiment began, the equipment was precisely calibrated to ensure that the collected point cloud three-dimensional coordinates accurately reflect the true dimensions of the real world. Additionally, manual measurements were taken of the phenotypic parameters such as leaf length, leaf width, leaf area, and stem length of the cotton seedlings. Accurate real values are crucial for validating and optimizing the algorithmic system framework. They not only ensure the reliability of the research results but also provide a basis for the continuous improvement and refinement of the algorithms.

To further enhance the accuracy of measurements, each plant's phenotypic parameters were measured three times, and the average of these measurements was used as the final data [24]. This practice effectively reduces the random errors that may arise from a single measurement and significantly improves the reliability and accuracy of the data. Additionally, this method does not cause damage to the plants from excessive measurements, thereby not affecting the progress of subsequent experiments.

2.3. The Overall Framework of the Method

The algorithm for extracting phenotypic parameters from cotton seedlings involves five main steps: point cloud collection, data preprocessing, data annotation, point cloud segmentation, and calculation of phenotypic parameters. Initially, the constructed point cloud data collection system is used to gather point cloud data from cotton seedlings. Subsequently, the collected data are preprocessed using conditional filtering, statistical filtering, and voxel filtering techniques to remove noise points. Next, the processed point clouds are annotated for training and testing purposes; cotton seedlings that require input into neural network training are labeled according to branches, stems, and leaves to create a dataset. For the cotton seedlings used in testing, different labels are assigned according to different organs to form a dataset for validating the performance of the segmentation algorithm. After data annotation, the initial cotton seedling point clouds without label information are input into a neural network-based cotton seedling organ segmentation algorithm for precise segmentation of the stem and leaf point clouds. Finally, phenotypic parameters are extracted from the segmented stem and leaf point clouds, and the feasibility of this method is verified. The overall framework of the method proposed in this article is shown in Figure 2.

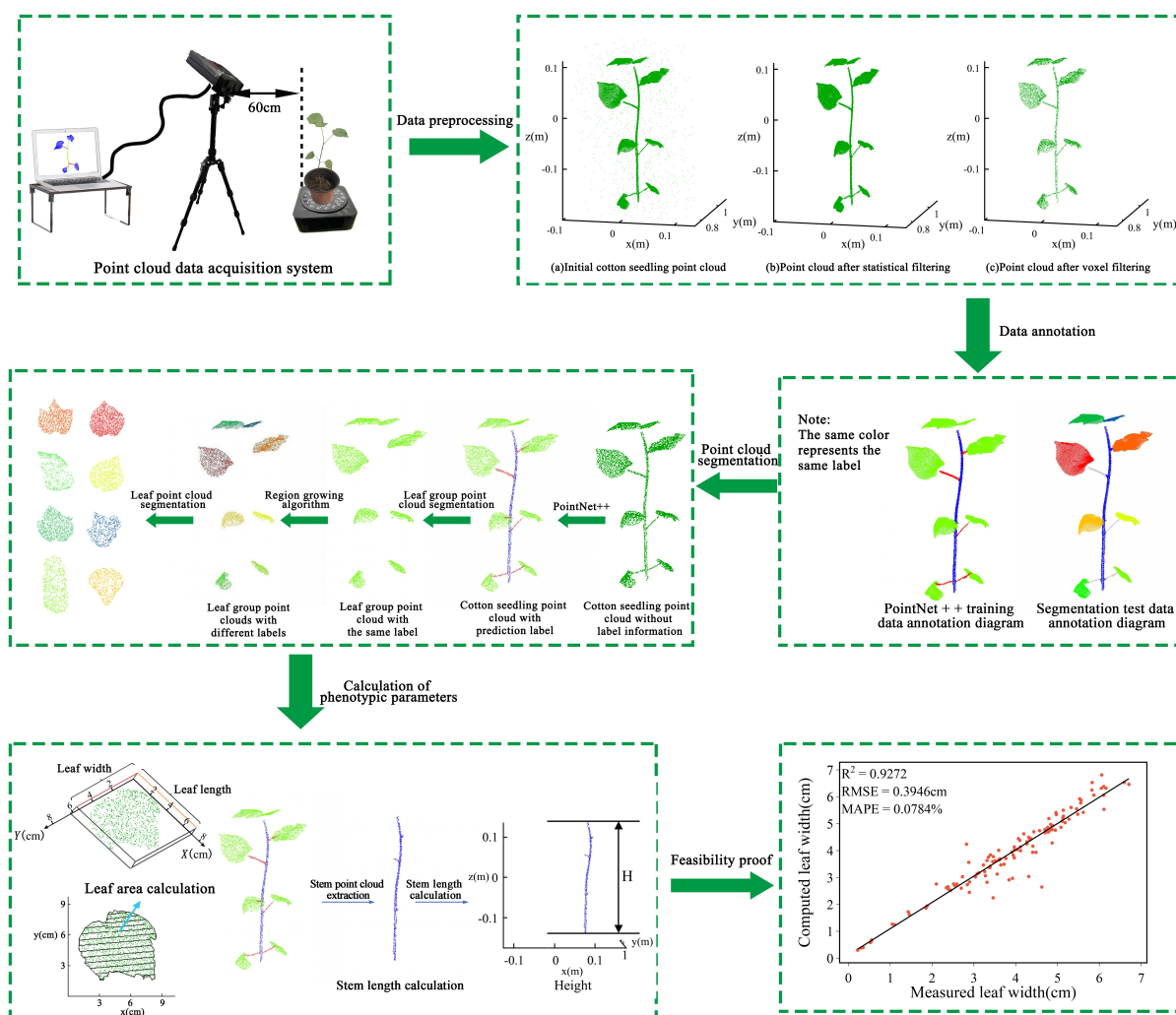


Figure 2. The overall framework diagram of the organ segmentation and phenotypic trait extraction method of cotton seedling point cloud based on a 3D lightweight network.

2.4. Cotton Seedling Point Cloud Data Preprocessing

2.4.1. Conditional Filtering

Point clouds contain a substantial amount of surrounding scene information. To remove irrelevant point clouds and extract the point cloud data of cotton seedlings from a complex background while preserving the detailed features of the seedlings, direct filtering and color thresholding techniques are used to isolate the cotton seedling point clouds. This provides a high-quality data foundation for subsequent analysis of phenotypic parameters. The results of conditional filtering processing are shown in Figure 3a.

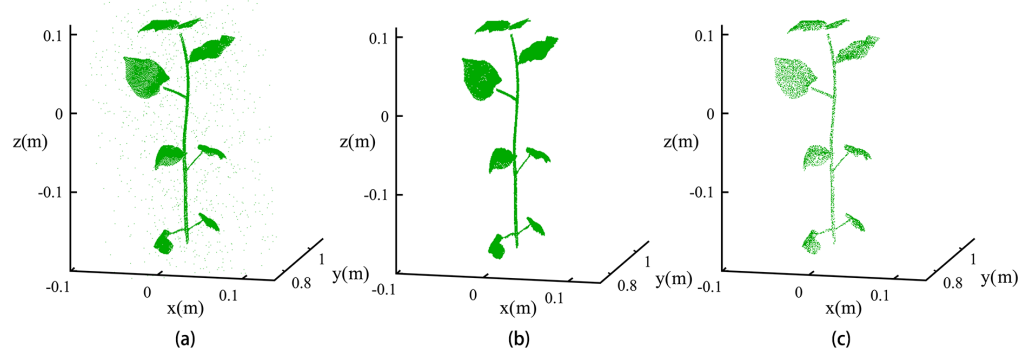


Figure 3. Preprocessing diagram of point cloud data: (a) cotton seedling point cloud after conditional filtering; (b) cotton seedling point cloud after statistical filtering; (c) cotton seedling point cloud after voxel filtering.

2.4.2. Statistical Filtering

Even after conditional filtering, there still exists a small number of noise points within the point cloud, which can affect subsequent point cloud segmentation and the calculation of phenotypic parameters. Outlier filtering is necessary to provide accurate point cloud information for further analysis, and any noise points that remain after filtering should be manually removed using CloudCompare v2.13.beta software to ensure the accuracy of the point cloud. Outlier filtering involves statistical analysis of each point p^i , calculating the average distance to m neighboring points. Assuming that the distance between a point and its neighbors follows a Gaussian distribution, the mean distance is μ_k , and then the standard deviation σ_k is calculated based on this. If a point's distance exceeds the defined range of standard distance, it can be considered an outlier. The specific formula is shown in Equation (1), where α^* is the standard deviation multiplier, and the smaller the multiplier, the more pronounced the effect. The results of the statistical filtering process are shown in Figure 3b.

$$p^* = \{ p^i \in P | \bar{d}_i \in [\mu_k - \alpha^* \sigma_k, \mu_k + \alpha^* \sigma_k] \} \quad (1)$$

2.4.3. Voxel Filtering

To enhance processing speed while ensuring accuracy, this experiment employed voxel filtering technology for downsampling the point cloud data. This method divides the space into cubes V_i with side length a . For each cube V_i , it aggregates the coordinate information of points inside, representing the center position of the cube V_i with the average coordinates of these points, and its volume is a^3 . This approach effectively reduces the number of points without compromising the overall shape features of the point cloud, thereby not adversely affecting subsequent phenotypic point cloud segmentation and parameter extraction. The specific formula is given in Equation (2). The results of voxel filtering processing are shown in Figure 3c.

$$p^i = \frac{1}{n} \sum_{k=1}^n (x^k, y^k, z^k)^T, (x^k, y^k, z^k)^T \in V_i \quad (2)$$

2.5. Organ Segmentation Algorithm for Cotton Seedlings

The segmentation of stems and leaves in plant point cloud data is a prerequisite for accurate trait measurement [25]. By employing a segmentation algorithm based on PointNet++ and region growing, precise segmentation of plant organs can be achieved, bridging the gap between point cloud data and cotton phenotypic parameter estimation, and enhancing the accuracy of phenotypic parameter estimation. The structural diagram of the cotton seedling organ segmentation algorithm is shown in Figure 4.

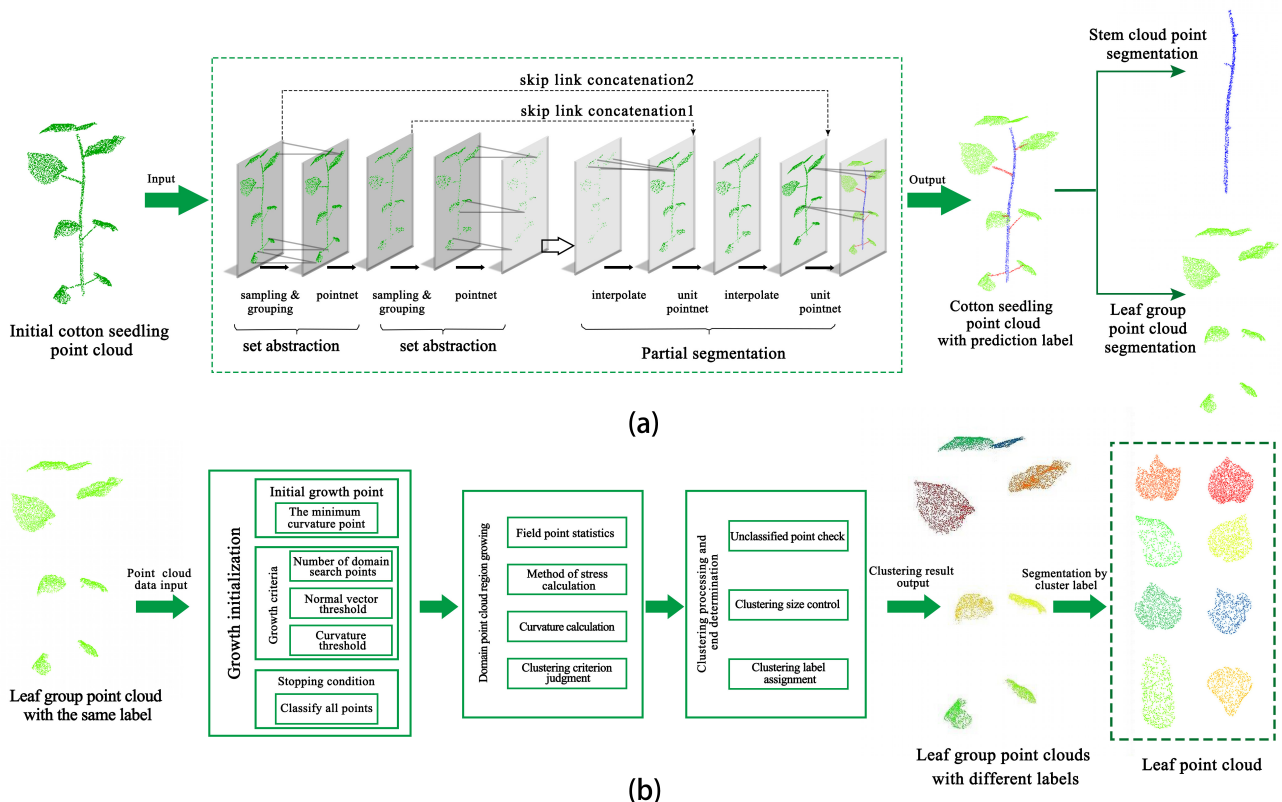


Figure 4. Structure diagram of cotton seedling organ segmentation: (a) network structure of cotton seedling stem and leaf segmentation based on PointNet++; (b) structure diagram of leaf segmentation based on improved region growing.

2.5.1. Data Annotation

The cotton seedling organ segmentation model, trained using neural networks, requires a large dataset. However, the preprocessed cotton seedling point clouds lack segmentation information, making them unsuitable for direct input into neural networks for model training. Therefore, the preprocessed point cloud data are labeled according to different plant phenotypic shapes to create a dataset.

When training neural network models, the more comprehensive and extensive the training data, the better the model performs. However, an excessively large dataset can also increase the computational load of training the network. The cotton seedling point clouds were segmented and labeled using CloudCompare v2.13.beta software to create the dataset. For this experiment, a total of 100 plant point cloud samples were selected, with 90% of these samples used as the training set for PointNet++ and the remaining 10% serving as the validation dataset. The classification labels for the training set are shown in Table 2, and the dataset annotation results are illustrated in Figure 5.

Table 2. Training dataset classification labels.

Label	Leaf	Stem	Branch	Others
L	Green	Blue	Red	Null

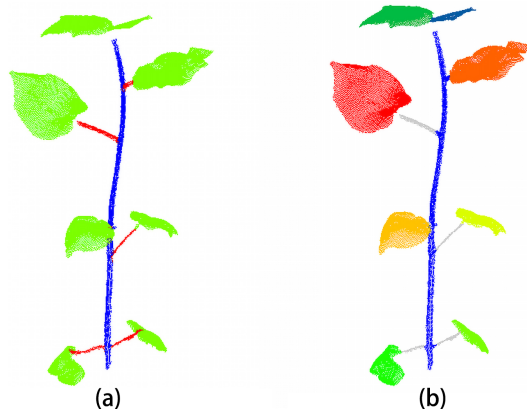


Figure 5. Dataset annotation result diagram: (a) PointNet++ training data annotation diagram; (b) segmentation test data annotation diagram.

2.5.2. Data Enhancement

To enhance the generalizability of the cotton seedling organ segmentation model, reduce the risk of overfitting, and improve the model's robustness, data augmentation steps were added to the collected cotton seedling point clouds. The data augmentation steps include data normalization, random rotation, and random jitter.

Data normalization involves converting the cotton seedling point clouds to the same scale, specifically through coordinate transformation and proportional stretching. The calculation formula is as follows:

Coordinate conversion:

$$p(x, y, z) = [x - \min(P_x) \quad y - \min(P_y) \quad z - \min(P_z)] \quad (3)$$

Isometric stretching:

$$p(x, y, z) = \left[\frac{100x}{\max(P_x)} \quad \frac{100y}{\max(P_y)} \quad \frac{100z}{\max(P_z)} \right] \quad (4)$$

Random rotation involves rotating the cotton seedling point cloud data around the z-axis by a random angle. The range of rotation is from 0 to 180 degrees. The calculation formula is as follows:

$$p(x, y, z) = [x \quad y \quad z] \begin{bmatrix} \cos\alpha & \sin\alpha & 0 \\ -\sin\alpha & \cos\alpha & 0 \\ 0 & 0 & 1 \end{bmatrix} \quad (5)$$

$$\alpha = \text{rand}(0, 180) \quad (6)$$

Random perturbation involves adding a random offset to the three-dimensional coordinates of the cotton seedling point cloud data. The offset is controlled within the range of 0 to 0.03 m. The calculation formula is as follows:

$$p(x, y, z) = [x \quad y \quad z] + \text{rand}(0, 0.05) \quad (7)$$

2.5.3. Stem and Leaf Point Cloud Separation

To achieve separation of the stem point cloud and leaf cluster point cloud, local features of the cotton seedling point cloud are extracted layer by layer through the set abstraction module of the PointNet++ neural network. The set abstraction module consists of a sampling layer, a grouping layer, and a feature extraction layer. The sampling layer utilizes farthest point sampling to select subsets of points, improving coverage of the entire point set. The grouping layer finds “neighboring” points around centroids, dividing the point cloud into multiple local point sets, thereby enhancing the spatial generalization of local features. The feature extraction layer employs a simplified PointNet, retaining only the multi-layer perceptron and max pooling, to extract features from the local point sets obtained in the grouping layer.

After extracting the local features, they are up-sampled using the feature transfer module. Subsequently, the sampled and unsampled points are spliced to minimize data loss caused by sampling and interpolation. Following this, the features undergo dimension reduction to match the number of categories. This process outputs the category probability of each point in the point cloud, thereby completing the segmentation of the cotton seedling stem and leaf cluster point cloud. The network structure of cotton seedling segmentation based on PointNet++ is illustrated in Figure 4a.

Aiming at the problem of disorder in a 3D point cloud, Charles R.Q. [26] proposed the use of symmetric functions to accommodate the replacement invariance of a 3D point cloud. The corresponding function mapping for the network structure is shown in (8):

$$f(\{P_1, P_2, \dots, P_n\}) \approx g(h(P_1), h(P_2), \dots, h(P_n)) \quad (8)$$

In the formula, $\{P_1, P_2, \dots, P_n\}$ is the target point cloud set, function mapping g is the maximum pooling function; and function mapping h is the feature extraction function.

2.5.4. Leaf Point Cloud Segmentation

An enhanced region-growing algorithm is employed to achieve the segmentation of leaf cluster point clouds. This algorithm merges points that are sufficiently close to each other and segments the leaf point clouds with similar features based on smoothness constraints, preserving edge information more effectively.

During the initialization phase of growth, the curvature is computed for each point in the input point cloud, and the point with the least curvature is chosen as the initial growth point. Selecting points with lower curvature aids in locating the flat surface of the plant leaf, as these points typically represent the starting point of the plant leaf, which is advantageous for the growth process.

In defining the growth criterion, a normal vector angle threshold is introduced in addition to the traditional region-growing algorithm. This addition enhances adaptation to the geometric and topological characteristics of leaf segmentation. Combined with the curvature threshold, it facilitates accurate identification and segmentation of leaves, providing more precise inputs for computing phenotypic parameters.

Furthermore, in the clustering processing and end decision stage, maximum and minimum values of clusters are established to ensure clustering quality and prevent the generation of excessively fine or large clusters, which could affect subsequent phenotypic parameter calculations. The leaf segmentation algorithm diagram based on improved region growing is shown in Figure 4b. The pseudocode of the improved curvature-based region-growing algorithm is shown below (Algorithm 1), which can make it more intuitive to understand the details of the algorithm.

Algorithm 1: Improved region-growing algorithm based on the curvature.

Input: P = cotton seedling individual point cloud
 θ = normal vector threshold
 k = curvature threshold

Output: result of leaf segmentation
the point P_i with the smallest curvature grows as the first seed point

for P_i in P **do**

- if** $P_{i\theta} < \theta$ **then**
- if** $P_{ik} < k$ **then**
grow into one category
- else**
continue to grow as a new seed point
- else**
discard

The Euclidean distance algorithm picks up the discarded points to the nearest category

In order to improve the speed of cluster segmentation, this experiment approximately calculates the local curvature of a certain point based on three consecutive points p_1 , p_2 , and p_3 . First, calculate the vectors $\vec{V}_1 = p_2 - p_1$ and $\vec{V}_2 = p_3 - p_2$. These two vectors represent the directions from point p_1 to point p_2 and from point p_2 to p_3 respectively. Then, calculate the cross-product $\vec{V}_{cross} = \vec{V}_1 \times \vec{V}_2$ of these two vectors. Finally, the curvature k is approximately calculated as follows:

$$k = \frac{|\vec{v}_{cross}|}{|\vec{v}_1||\vec{v}_2|} \quad (9)$$

2.5.5. The Model Training and Configurations

Experimental Configuration. The experiment was conducted using the following setup: an AMD Ryzen 9 5900HX CPU (Advanced Micro Devices, Inc., Santa Clara, CA, USA), 16 GB of memory, and an NVIDIA GeForce RTX 3060 (NVIDIA Corporation, Santa Clara, CA, USA) graphics card. The system operated on Windows 10 (Microsoft, USA) with a configured Python 3.7 programming environment, CUDA architecture, and cuDNN development library. Model building, training, and network prediction were performed under this setup using the deep learning framework PyTorch.

Training Strategy. The training parameters were as follows: a weight decay rate of 0.0001, an initial learning rate of 0.001, a total of 251 iterations, a learning rate decay factor of 0.5, and a learning rate adjustment step size of 20. The cross-entropy loss function [27], indicated in Equation (10), was utilized for network optimization, along with the AdamW optimizer [28] to enhance the process. The training duration was 5.6 h, achieving a maximum accuracy of 0.9886 on the training set and 0.9873 on the test set.

$$\text{Loss} = \sum_{i=1}^m -(y_i \log(p_i) + (1 - y_i) \log(1 - p_i)) \quad (10)$$

2.6. Calculation of Phenotypic Parameters in Cotton Seedlings

Plant phenotypic parameters extracted from segmented stem and leaf point cloud data, such as stem length, leaf length, leaf width, and leaf area, are essential for assessing the growth and health of cotton seedlings. These parameters not only reflect the growth rate and biomass accumulation of the plant but also reveal the plant's adaptability and physiological responses to environmental changes.

2.6.1. Stem Length Calculation Method

Stem length is a critical indicator for measuring plant growth, which can vary significantly due to environmental conditions. Generally, plant height is determined by measuring the vertical distance between the highest and lowest points of the plant [29]. The calculation formula is as follows (11):

$$H = z_{max} - z_{min} \quad (11)$$

where H is the calculated plant height, z_{max} is the maximum value in the z -axis direction, and z_{min} is the minimum value in the z -axis direction. The schematic diagram of the plant height calculation is shown in Figure 6.

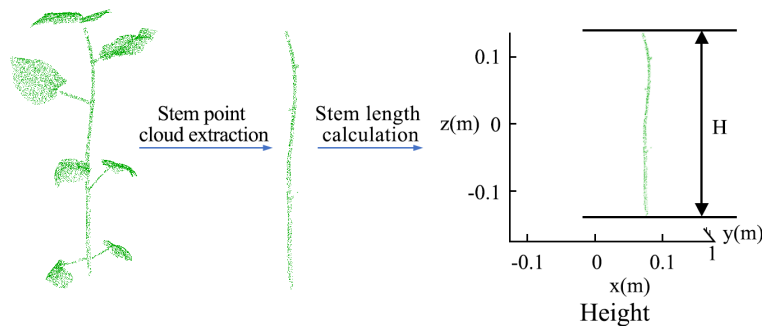


Figure 6. Stem length calculation diagram.

2.6.2. Leaf Length Calculation Method

First, the coordinate correction of the leaf point cloud is performed based on the principal component analysis method, calculating its three principal component axes. Among these, the shortest path between the two endpoints of the first principal component is referred to as the leaf length path, and the length of this path is calculated using the Euclidean distance formula to extract the leaf length parameter [30]. The Euclidean distance formula is as follows:

$$d = \sqrt{(x_2 - x_1)^2 + (y_2 - y_1)^2 + (z_2 - z_1)^2} \quad (12)$$

2.6.3. Leaf Width Calculation Method

In the point cloud data, the shortest path T_1 connecting the two endpoints of the second principal component axis is first extracted. Then, the shortest path T_2 connecting the two endpoints of the third principal component axis is identified. The longest path between T_1 and T_2 is considered the leaf width path, and its length is used as the leaf width parameter [30]. The calculation of leaf length and leaf width is illustrated in Figure 7.

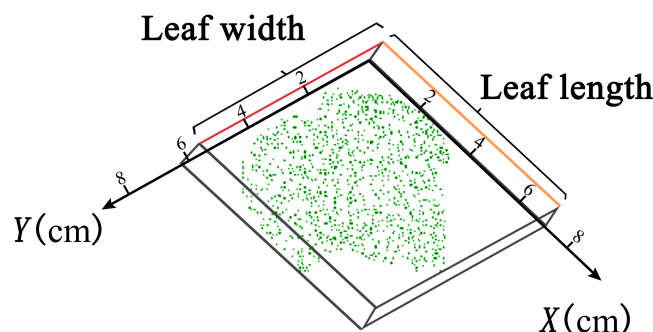


Figure 7. Calculation diagram of leaf length and leaf width.

2.6.4. Leaf Area Calculation Method

Leaves, as the primary organs for photosynthesis in plants, play a crucial role in plant growth and development. To accurately determine leaf area, this paper proposes a method based on leaf point cloud data and the rolling ball radius for creating a triangular mesh. The rolling ball radius technique is an effective mesh generation method that precisely determines the vertices and boundaries of the mesh by simulating the rolling process of a sphere on the surface of the point cloud. The specific mesh generation process is as follows:

$$M = \bigcup_{i=1}^N T(p_i, r) \quad (13)$$

where M represents the generated mesh, p_i denotes a point in the point cloud, r is the rolling ball radius, and $T(p_i, r)$ represents the local triangular mesh generated by a sphere centered at p_i with radius r .

After the mesh is computed, the total surface area of the leaf can be obtained by summing the areas of each triangle. Specifically, let S_i be the area of the i -th triangle, then the total leaf area A can be expressed as follows:

$$A = \sum_{i=1}^k S_i \quad (14)$$

where k represents the total number of triangles. The area of each triangle can be calculated using Heron's formula, as follows:

$$S = \sqrt{p \times (p - a) \times (p - b) \times (p - c)} \quad (15)$$

where S is the area of the triangle, p is the semi-perimeter, calculated as $p = \frac{a+b+c}{2}$, and a , b , and c are the lengths of the sides of the triangle. An illustrative diagram of the leaf area calculation is shown in Figure 8.

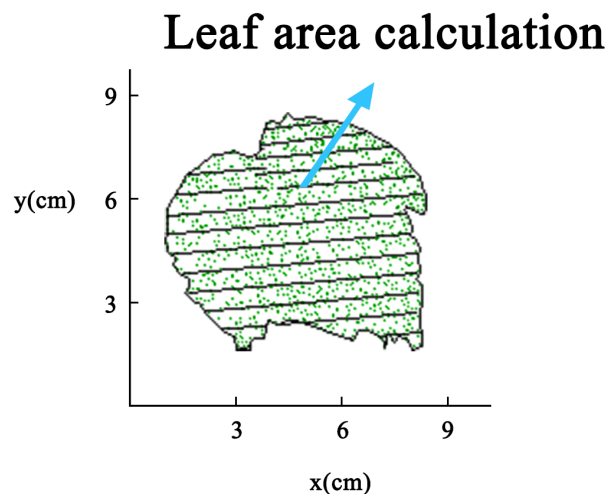


Figure 8. Calculation diagram of leaf area.

3. Results

3.1. Evaluation Indicators

The evaluation metrics used in this paper are calculated based on the confusion matrix. The single-category dichotomous confusion matrix is shown below.

In Table 3, T_p is a true case, which means that the prediction is a positive sample and the instance is also a positive sample; F_p is a false positive case, which means that the prediction is a positive sample but the instance is a negative sample; F_N is a false negative

case, which means that the prediction is a negative case but it is actually a positive case; and T_N is a true negative case, which means that the prediction is a negative case and it is actually a negative case.

Table 3. Confusion matrix.

		Estimate	
		True	False
Actual value	True	True Positives (T_p)	False Negatives (F_N)
	False	False Positives (F_p)	True Negatives (T_N)

In order to verify the segmentation effect, the precision (p_{re}), recall (r_{ec}), F_1 score, and the intersection of union (I_{IoU}) are introduced as the evaluation indexes, which are calculated as follows:

$$p_{re} = \frac{T_p}{T_p + F_p} \quad (16)$$

$$r_{ec} = \frac{T_p}{T_p + F_N} \quad (17)$$

$$F_1 = 2 \times \frac{p_{re} r_{ec}}{p_{re} + r_{ec}} \quad (18)$$

Precision (p_{re}) indicates the proportion of samples predicted to be positive that is actually positive; Recall (r_{ec}) indicates the proportion of samples correctly predicted to be positive among all positive samples; and the F_1 score is the reconciled average of the precision and recall. The intersection of union (I_{IoU}) is the ratio of the intersection and concatenation of the true value and the predicted value of a category. The formula for calculating I_{IoU} is shown in Equation (19):

$$I_{IoU} = \frac{N_{Class-R} \cap N_{Class-P}}{N_{Class-R} \cup N_{Class-P}} \quad (19)$$

where $N_{Class-R}$ is the number of points that actually belong to the class, and $N_{Class-P}$ is the number of points predicted by the model to be in that class.

In order to validate the calculations of the phenotypic parameters, linear regression analysis was used to evaluate the relationship between the manually measured values of the phenotypic parameters and the extracted ones. The coefficient of determination (R^2), root mean square error ($RMSE$), and mean percentage error ($MAPE$) were used for quantitative assessment [31]. The formulas were calculated as follows:

$$RMSE = \sqrt{\frac{1}{n} \sum_{i=1}^n (x_{ci} - x_{mi})^2} \quad (20)$$

$$MAPE = \frac{1}{n} \sum_{i=1}^n \frac{|x_{ci} - x_{mi}|}{x_{mi}} \times 100\% \quad (21)$$

$$R^2 = 1 - \frac{\sum_{i=1}^n (x_{ci} - x_{mi})^2}{\sum_{i=1}^n x_{ci}^2} \quad (22)$$

where x_{ci} represents the actual value of the i , x_{mi} represents the predicted value of the model for the i , and n represents the number of actual values.

3.2. Analysis of Organ Segmentation Results in Cotton Seedlings

The cotton seedling organ segmentation algorithm proposed in this paper visualizes the segmentation results for different cotton varieties, as shown in Figure 9. This visualization method intuitively presents the segmentation efficacy of the algorithm, providing a

valid basis for evaluation. From the images, it can be observed that the algorithm accurately segments the organ point clouds of both cotton seedling varieties, and the number of stems and leaves conforms to the expected targets.



Figure 9. Visualization of segmentation results for different cotton seedling varieties: (a) Visualization of cotton segmentation results of Xinluzao 1 variety; (b) Visualization map of segmentation results of Xinluzao 76 variety.

To further quantify the segmentation accuracy of the algorithm, ten plants each of Xinluzao 1 and Xinluzao 76 cotton varieties were selected as test samples. Table 4 details the segmentation evaluation results for these samples. For the two different cotton varieties, the average precision, recall, F_1 score, and intersection over union (I_{IoU}) were, respectively, as high as 96.67%, 94.32%, 95.42%, 91.66%, 93.4%, 91.95%, 92.48%, and 86.79%. This fully demonstrates the applicability of the segmentation algorithm based on PointNet++ and region growing to different varieties of cotton seedlings. It effectively extracts key phenotypic organs from point cloud data, and the segmentation results are closer to the actual shape.

Table 4. Segmentation results of different cotton seedlings based on PointNet++ and improved the region-growing segmentation algorithm.

Variety of Cotton	Average Precision	Average Recall	Average F_1 Score	Average I_{IoU}
Xinluzao 1	0.9667	0.9432	0.9542	0.9166
Xinluzao 76	0.9340	0.9195	0.9248	0.8679

This study compares the segmentation algorithm based on PointNet++ and improved region growing (PRG-Net) used with other typical point cloud segmentation methods, including a DFSP segmentation [32], a density-based spatial clustering algorithm (DBSCAN) [33] and a clustering algorithm based on Euclidean distances (Euclidean Clustering) [34]. The specific comparison results, as shown in Table 5, indicate that across 10 test samples, the average precision of the algorithm in this paper reaches 96.67%, while the average precision of the other three algorithms are 75.4%, 70.33%, and 68.4%, respectively. The results demonstrate that the segmentation efficacy of the algorithm in this paper is significantly higher than in other point cloud segmentation methods, exhibiting superior segmentation precision.

Table 5. Comparison of segmentation results of different algorithms. PRG-Net: Segmentation algorithm based on PointNet++ and improved region growth (proposed in this study); DFSP: DFSP segmentation; DBSCAN: density-based spatial clustering algorithm; Euclidean clustering: clustering algorithm based on Euclidean distances.

Segmentation Algorithm	Average Precision	Average Recall	Average F_1 Score	Average I_{IoU}
PRG-Net	0.9667	0.9432	0.9542	0.9166
DFSP	0.7540	0.7119	0.7132	0.7006
DBSCAN	0.7033	0.7832	0.7093	0.7213
Euclidean Clustering	0.6840	0.6652	0.6724	0.6535

The bold font indicates the current optimal value.

Figure 10 shows the comparison of segmentation results using four different algorithms. The neural network-based cotton seedling organ segmentation algorithm proposed in this paper accurately distinguishes the four leaves and the stem. In contrast, the DFSP segmentation [32] incorrectly segments the left leaf into three clusters; the density clustering algorithm [33] merges the top two leaves into one cluster; the Euclidean distance clustering algorithm [34] splits the largest leaf on the right into two clusters. Moreover, these three algorithms perform poorly in extracting stems because the branches and stems of the plant are closely connected, and traditional unsupervised learning methods struggle to effectively extract stem point cloud data. The results demonstrate that the cotton seedling phenotypic organ segmentation algorithm developed in this study exhibits higher robustness in the segmentation of cotton seedling point clouds.

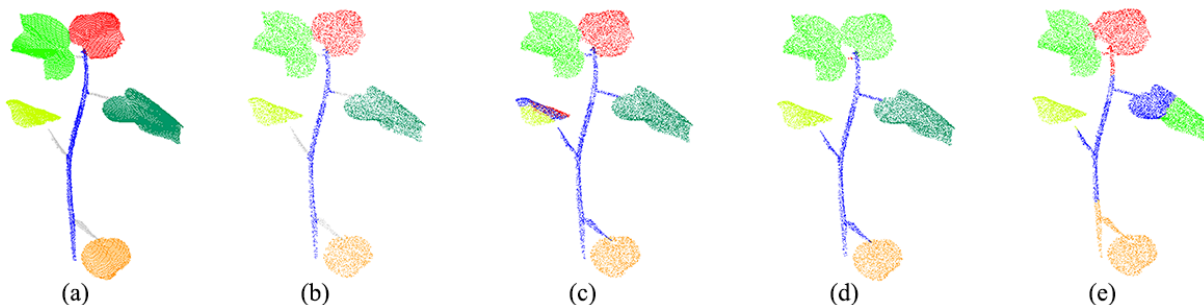


Figure 10. Visualization of the segmentation results of four methods for cotton seedlings: (a) Real value of manual segmentation; (b) segmentation algorithm based on PointNet++ and improved region growing; (c) DFSP segmentation; (d) density-based spatial clustering algorithm; (e) clustering algorithm based on Euclidean distances.

3.3. Analysis of the Results of Calculating Phenotypic Parameters of Cotton Seedlings

By comparing automatically acquired three-dimensional phenotypic features, such as stem length, leaf area, and leaf perimeter, with actual values, the accuracy of the results is calculated using three metrics: root mean square error ($RMSE$), mean absolute percentage error ($MAPE$), and R^2 . The calculation formulas are shown in (20)–(22). Figure 11a–d displays the linear correlation between computed and measured values of cotton seedling stem length, leaf length, leaf width, and leaf area, with R^2 values of 91.97%, 90.70%, 92.72%, and 95.44%, respectively. According to Equation (20), the ($RMSE$) values for cotton seedling stem length, leaf length, leaf width, and leaf area are 1.9659 cm, 0.3998 cm, 0.3946 cm, and 4.6306 cm², respectively. According to Equation (22), the ($MAPE$) values are 0.0688%, 0.0599%, 0.0784%, and 0.2203%, respectively. The results show a significant linear correlation between the calculated phenotypic parameters of cotton seedlings and the actual measurements, with an average coefficient of determination of 92.71% and an average percentage error of 0.1069%. This algorithm can quickly and accurately calculate

the phenotypic parameters of cotton seedlings, addressing the issues of low efficiency and inaccuracy in traditional agricultural measurements.

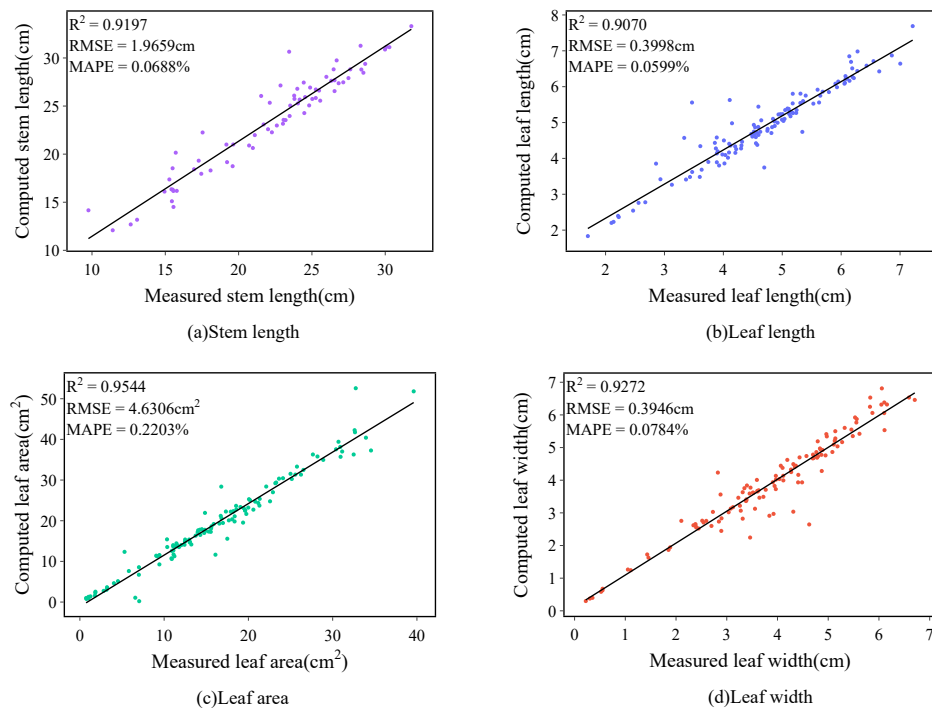


Figure 11. Graph of phenotypic parameter measurement results.

4. Discussion

Traditional methods for measuring seedling phenotypic parameters rely on manual operations, which are cumbersome and inefficient and may also damage the plants. Therefore, this paper proposes a cotton seedling phenotypic parameter extraction algorithm based on point cloud segmentation. This algorithm precisely segments the stem and leaf organs in the plant point cloud data, and then calculates key phenotypic parameters such as stem length, leaf length, leaf width, and leaf area. The results are compared and analyzed against real values to verify the effectiveness and accuracy of the algorithm. Finally, based on this algorithm, a cotton seedling phenotypic parameter analysis system was developed. This system can efficiently and accurately extract key phenotypic parameters of plants, providing robust technical support and tools for breeding experts and researchers in the field of agronomy. The discussion is as follows:

Obtaining high-precision cotton seedling point clouds is a prerequisite for extracting phenotypic parameters. This paper demonstrates that the binocular reconstruction instrument can efficiently, conveniently, and accurately capture the three-dimensional phenotypic information of plants. Compared to traditional methods based on 2D images, it addresses inaccuracies in the feature representation of cotton seedlings due to size limitations and highlights the advantages of depth information in describing the spatial form of plants. Compared to using single-view image capture technology [35], it compensates for incomplete point cloud information caused by occlusion from plant leaves or stems, which previously hindered accurate phenotypic information acquisition, thus enhancing the accuracy and completeness of plant point cloud data collection. During the point cloud acquisition process, by controlling the speed of the turntable and filtering out outliers, experimental errors caused by plant movement are minimized, further improving the precision of the overall point cloud.

Accurate segmentation of plant stems and leaves is crucial for precisely measuring phenotypic parameters associated with different organs [24]. A neural network-based segmentation algorithm for cotton seedling organs is proposed, which shows higher adapt-

ability compared to the unsupervised DFSP segmentation algorithm [32]. It directly extracts features from raw data and completes the segmentation task through end-to-end learning. This algorithm performs excellently under complex data and scenarios, showing significant improvements over the DFSP segmentation in terms of average precision, recall, F_1 score, and intersection over union (I_{IoU}), with increases of 0.2127, 0.2313, 0.2410, and 0.2160, respectively, achieving high-precision segmentation of cotton seedlings. When managing large-scale point cloud data, the segmentation algorithm—based on PointNet++ and an improved region-growing method—acts as a lightweight neural network, demonstrating high computational efficiency and outstanding segmentation performance. In segmentation tests conducted on ten cotton seedlings, the average segmentation time was about 1.6 s. Although this is slower than traditional unsupervised algorithms, the proposed algorithm significantly surpasses these in terms of segmentation accuracy, effectively compensating for the time deficit, and can achieve efficient and precise segmentation of key phenotypic organs in large-scale plant point cloud data.

Through meticulous processing of point cloud data from cotton seedlings, we have successfully achieved precise segmentation of cotton organs and calculated key phenotypic parameters such as stem length, leaf length, leaf width, and leaf area. Notably, there exists a significant linear correlation between the calculated values and the actual measurements, indicating low error rates. This method not only eliminates the potential for damage and errors associated with traditional manual measurements but also significantly improves measurement efficiency and accuracy. It provides powerful technical support for cotton breeding research and plant phenotyping calculations.

5. Conclusions

This paper presents an organ segmentation and phenotypic trait extraction of cotton seedling point clouds based on a 3D lightweight network, capable of achieving precise organ segmentation and automated calculation of phenotypic parameters. Initially, the collected point clouds are preprocessed using conditional filtering, statistical filtering, and voxel filtering to effectively remove noise and extract cotton seedling point clouds. Then, the neural network-based cotton seedling organ segmentation algorithm is used for stem and leaf point cloud segmentation. Compared to the average precision of 75.4% with the DFSP segmentation [32], the segmentation algorithm proposed in this paper achieves an average precision of 96.67%, realizing excellent segmentation of cotton seedlings. The calculated values of phenotypic parameters such as stem length, leaf length, leaf width, and leaf area have an average coefficient of determination R^2 of 92.71%, with the maximum root mean square error (RMSE) reaching only 4.6306 cm² and a mean percentage error (MAPE) of 0.1069%, ensuring the precision of the extracted phenotypic information from cotton seedlings. The results indicate that the point cloud segmentation and phenotypic parameter calculation methods used in this experiment are highly robust and adaptive, capable of achieving precise segmentation and phenotypic information extraction for plant organs of different morphologies. This method significantly alleviates the workload of breeding experts and enhances the efficiency of phenotypic parameter extraction, providing robust technical support for scientific research and practical applications in the field of agriculture.

Furthermore, the application of this model can be further expanded, such as measuring and analyzing phenotypic information at different growth stages of plants, establishing growth prediction models, and investigating the mechanisms by which environmental factors affect plant growth, providing a scientific basis for crop breeding and cultivation management. In application areas, this technology can be extended to the monitoring and management of farmlands. By integrating various data sources such as drones and ground sensors, a complete smart agriculture system can be constructed. This system enables real-time monitoring, data analysis, and decision support for agricultural environments, thereby promoting the intelligent and modern advancement of agricultural production.

Author Contributions: Conceptualization, J.S. and P.G.; methodology, J.S. and P.G.; software, J.S., T.W., J.Z. and Y.H.; validation, J.S., Z.W. and Y.H.; formal analysis, J.S., T.W. and J.Z.; investigation, T.W., J.Z. and Y.H.; resources, J.Z., Z.W., Y.H. and P.G.; data curation, J.S., J.Z. and Y.H.; writing—original draft preparation, J.S., T.W. and Z.W.; writing—review and editing, J.S. and P.G.; visualization, J.S. and J.Z.; supervision, P.G. and L.Z.; project administration, J.S., P.G. and L.Z.; funding acquisition, J.S. and P.G. All authors have read and agreed to the published version of the manuscript.

Funding: This study was financially supported by the XPCC Youth Science and Technology Innovation Talents Project (2023CB008-16); the National Training Program of Innovation and Entrepreneurship for Undergraduates (202310759050), and the Scientific and Technological Achievements Transformation project of Shihezi University (CGZH202310).

Data Availability Statement: All data can be obtained by email from the corresponding author.

Conflicts of Interest: The authors declare no conflicts of interest.

References

1. Ge, X.; Xu, J.; Yang, Z.; Yang, X.; Wang, Y.; Chen, Y.; Wang, P.; Li, F. Efficient genotype-independent cotton genetic transformation and genome editing. *J. Integr. Plant Biol.* **2023**, *65*, 907–917. [CrossRef] [PubMed]
2. Abdelraheem, A.; Esmaeili, N.; O’Connell, M.; Zhang, J. Progress and perspective on drought and salt stress tolerance in cotton. *Ind. Crop. Prod.* **2019**, *130*, 118–129. [CrossRef]
3. Ministry of Agriculture and Rural Affairs Expert Committee on Agricultural Trade Warning and Relief. International agricultural market price and trade situation monthly report. *World Agric.* **2023**, *9*, 125–128.
4. Li, N.; Lin, H.; Wang, T.; Li, Y.; Liu, Y.; Chen, X.; Hu, X. Impact of climate change on cotton growth and yields in Xinjiang, China. *Field Crop. Res.* **2020**, *247*, 107590. [CrossRef]
5. Lu, X.; Jia, X.; Niu, J. Current situation and prospect of China’s cotton industry. *Chin. Agric. Sci.* **2018**, *51*, 26. [CrossRef]
6. Hu, J.; Wang, M.; Li, T.; Wu, D.; Tian, D. Automatic observation of cotton development period based on deep learning. *J. Anhui Agric. Sci.* **2019**, *47*, 237–240+243. [CrossRef]
7. Xu, S.; Li, L.; Tong, H.; Wang, C.; Bie, Z.; Huang, Y. Research on 3D phenotype high-throughput measurement system of cucumber seedlings based on RGB-D camera. *Trans. Chin. Soc. Agric. Mach.* **2023**, *54*, 204–213. [CrossRef]
8. Gupta, P.K.; Rustgi, S.; Kulwal, P.L. Linkage disequilibrium and association studies in higher plants: Present status and future prospects. *Plant Mol. Biol.* **2005**, *57*, 461–485. [CrossRef] [PubMed]
9. Zhang, W.; Li, X.; Wan, H.; Li, C.; Zhang, W.; Jin, B.; Liu, Y. Maize plant image stem-leaf segmentation method based on skeleton extraction and binary tree analysis. *Henan Agric. Sci.* **2020**, *49*, 7. [CrossRef]
10. Bylesjö, M.; Segura, V.; Soolanayakanahally, R.Y.; Rae, A.M.; Trygg, J.; Gustafsson, P.; Jansson, S.; Street, N.R. LAMINA: A tool for rapid quantification of leaf size and shape parameters. *BMC Plant Biol.* **2008**, *8*, 1–9. [CrossRef]
11. Dhondt, S.; Wuyts, N.; Inzé, D. Cell to whole-plant phenotyping: The best is yet to come. *Trends Plant Sci.* **2013**, *18*, 428–439. [CrossRef]
12. Lee, U.; Chang, S.; Putra, G.A.; Kim, H.; Kim, D.H. An automated, high-throughput plant phenotyping system using machine learning-based plant segmentation and image analysis. *PloS ONE* **2018**, *13*, e0196615. [CrossRef]
13. Ji, Y.; Chen, Z.; Cheng, Q.; Liu, R.; Li, M.; Yan, X.; Li, G.; Wang, D.; Fu, L.; Ma, Y.; et al. Estimation of plant height and yield based on UAV imagery in faba bean (*Vicia faba* L.). *Plant Methods* **2022**, *18*, 26. [CrossRef]
14. Minervini, M.; Scharr, H.; Tsafaris, S.A. Image analysis: The new bottleneck in plant phenotyping [applications corner]. *IEEE Signal Process. Mag.* **2015**, *32*, 126–131. [CrossRef]
15. Gibbs, J.A.; Pound, M.; French, A.P.; Wells, D.M.; Murchie, E.; Pridmore, T. Approaches to three-dimensional reconstruction of plant shoot topology and geometry. *Funct. Plant Biol.* **2016**, *44*, 62–75. [CrossRef]
16. Miao, T.; Zhu, C.; Xu, T.; Yang, T.; Li, N.; Zhou, Y.; Deng, H. Automatic stem-leaf segmentation of maize shoots using three-dimensional point cloud. *Comput. Electron. Agric.* **2021**, *187*, 106310. [CrossRef]
17. Wang, C.; Zhao, M.; Yan, J.; Zhou, S.; Zhang, Y. Three-dimensional reconstruction of corn leaves based on binocular stereo vision technology. *Trans. Chin. Soc. Agric. Eng.* **2010**, *4*, 26.
18. Lai, Y.; Lu, S.; Qian, T.; Song, Z.; Chen, M. Plant three-dimensional point cloud segmentation. *J. Appl. Sci.* **2021**, *39*, 660. [CrossRef]
19. Gehan, M.A.; Fahlgren, N.; Abbasi, A.; Berry, J.C.; Callen, S.T.; Chavez, L.; Doust, A.N.; Feldman, M.J.; Gilbert, K.B.; Hodge, J.G.; et al. PlantCV v2: Image analysis software for high-throughput plant phenotyping. *PeerJ* **2017**, *5*, e4088. [CrossRef]
20. Chen, D.; Neumann, K.; Friedel, S.; Kilian, B.; Chen, M.; Altmann, T.; Klukas, C. Dissecting the phenotypic components of crop plant growth and drought responses based on high-throughput image analysis. *Plant Cell* **2014**, *26*, 4636–4655. [CrossRef]
21. Li, S.; Zhang, A.; Zhang, X.; Yang, Z.; Li, M. Method for extracting three-dimensional phenotype information of maize seedlings at leaf scale. *Laser Optoelectron. Prog.* **2023**, *60*, 210002. [CrossRef]
22. Li, N.; Lopez-Sanchez, J.M.; Fu, H.; Zhu, J.; Han, W.; Xie, Q.; Hu, J.; Xie, Y. Rice crop height inversion from TanDEM-X PolInSAR data using the RVoG model combined with the logistic growth equation. *Remote Sens.* **2022**, *14*, 5109. [CrossRef]

23. Li, S.; Zhu, Y.; Liu, H.; Li, S.; Liu, S.; Zhang, H.; Gao, W. Simulation of three-dimensional morphology of winter wheat plants after greening based on effective accumulated temperature. *Chin. Agric. Sci.* **2017**, *50*, 1594–1605. [[CrossRef](#)]
24. Ma, X.; Wei, B.; Guan, H.; Cheng, Y.; Zhuo, Z. A method for calculating and simulating phenotype of soybean based on 3D reconstruction. *Eur. J. Agron.* **2024**, *154*, 127070. [[CrossRef](#)]
25. Miao, Y.; Peng, C.; Wang, L.; Qiu, R.; Li, H.; Zhang, M. Measurement method of maize morphological parameters based on point cloud image conversion. *Comput. Electron. Agric.* **2022**, *199*, 107174. [[CrossRef](#)]
26. Qi, C.R.; Yi, L.; Su, H.; Guibas, L.J. PointNet++: Deep hierarchical feature learning on point sets in a metric space. *Adv. Neural Inf. Process. Syst.* **2017**, *30*. [[CrossRef](#)]
27. Huang, C.; Li, Y.; Loy, C.C.; Tang, X. Learning deep representation for imbalanced classification. *Proc. IEEE Conf. Comput. Vis. Pattern Recognit.* **2016**, 5375–5384. [[CrossRef](#)]
28. Loshchilov, I.; Hutter, F. Decoupled weight decay regularization. *arXiv* **2017**, arXiv:1711.05101. Available online: <https://arxiv.org/abs/1711.05101> (accessed on 15 May 2024).
29. Feng, J.; Ma, X.; Guan, H.; Zhu, K.; Yu, S. Calculation method of soybean plant height based on depth information. *Acta Opt. Sin.* **2019**, *39*, 515003. [[CrossRef](#)]
30. Zhu, C.; Miao, T.; Xu, T.; Li, N.; Deng, H.; Zhou, Y. Segmentation and phenotypic trait extraction of maize point cloud stem-leaf based on skeleton and optimal transportation distances. *Trans. Chin. Soc. Agric. Eng.* **2021**, *37*, 188–198. [[CrossRef](#)]
31. Wang, R.; Liu, D.; Xian, L.; Yang, H. Segmentation and measurement of key phenotype for Chinese cabbage sprout using multi-view geometry. *Trans. Chin. Soc. Agric. Eng.* **2022**, *38*, 243–251. [[CrossRef](#)]
32. Wang, D.; Miao, T.; Xu, T. DFSP: A fast and automatic distance field-based stem-leaf segmentation pipeline for point cloud of maize shoot. *Front. Plant Sci.* **2023**, *14*, 1109314. [[CrossRef](#)] [[PubMed](#)]
33. Elnashef, B.; Filin, S.; Lati, R.N. Tensor-based classification and segmentation of three-dimensional point clouds for organ-level plant phenotyping and growth analysis. *Comput. Electron. Agric.* **2019**, *156*, 51–61. [[CrossRef](#)]
34. Zermas, D.; Morellas, V.; Mulla, D.; Papanikopoulos, N. 3D model processing for high throughput phenotype extraction—The case of corn. *Comput. Electron. Agric.* **2020**, *172*, 105047. [[CrossRef](#)]
35. Zhu, K.; Ma, X.; Guan, H.; Feng, J.; Zhang, Z.; Yu, S. A method of calculating the leafstalk angle of the soybean canopy based on 3D point clouds. *Int. J. Remote Sens.* **2021**, *42*, 2463–2484. [[CrossRef](#)]

Disclaimer/Publisher’s Note: The statements, opinions and data contained in all publications are solely those of the individual author(s) and contributor(s) and not of MDPI and/or the editor(s). MDPI and/or the editor(s) disclaim responsibility for any injury to people or property resulting from any ideas, methods, instructions or products referred to in the content.